HHS Public Access

Author manuscript

Clin Biomech (Bristol, Avon). Author manuscript; available in PMC 2018 November 01.

Published in final edited form as:

Clin Biomech (Bristol, Avon). 2017 November ; 49: 101–106. doi:10.1016/j.clinbiomech.2017.09.005.

Analysis of In-vivo Articular Cartilage Contact Surface of the Knee during a Step-up Motion

Peng Yin[1,2], **Jing-Sheng Li**[1], **Willem A. Kernkamp**[1], **Tsung-Yuan Tsai**[1], **Seung-Hoon Baek**[1], **Ali Hosseini**[1], **Lin Lin**[3], **Peifu Tang**[4], and **Guoan Li**[1,*]

[1]Orthopaedic Biomechanics Laboratory, Harvard Medical School and Massachusetts General Hospital, Boston, MA, 02114, USA

[2]Department of Orthopaedics, Beijing Chao-Yang Hospital, China Capital Medical University, No. 8 GongTiNanLu, Chao-Yang District, Beijing, 100020, China

[3]Institute of Sports Medicine, Peking University Third hospital, North Garden Road, Haidian District, Beijing, 100191, PR China

[4]Department of Orthopaedics, Chinese PLA General Hospital, No. 28 Fuxin Road, Beijing 100853, P.R. China

Abstract

Background—Numerous studies have reported on the tibiofemoral articular cartilage contact kinematics, however, no data has been reported on the articular cartilage geometry at the contact area. This study investigated the in-vivo tibiofemoral articular cartilage contact biomechanics during a dynamic step-up motion.

Methods—Ten healthy subjects were imaged using a validated magnetic resonance and dual fluoroscopic imaging technique during a step-up motion. Three-dimensional bone and cartilage models were constructed from the magnetic resonance images. The cartilage contact along the motion path was analyzed, including cartilage contact location and the cartilage surface geometry at the contact area.

Findings—The cartilage contact excursions were similar in anteroposterior and mediolateral directions in the medial and lateral compartments of the tibia plateau ($p>0.05$). Both medial and lateral compartments were under convex (femur) to convex (tibia) contact in the sagittal plane, and under convex (femur) to concave (tibia) contact in the coronal plane. The medial tibial articular contact radius was larger than the lateral side in the sagittal plane along the motion path ($P<0.001$).

Interpretations—These data revealed that both the medial and lateral compartments of the knee experienced convex (femur) to convex (tibia) contact in sagittal plane (or anteroposterior direction) during the dynamic step-up motion. These data could provide new insight into the in-vivo cartilage

*CORRESPONDING AUTHOR. Guoan Li, Orthopaedic Biomechanics Laboratory, Harvard Medical School and Newton-Wellesley Hospital, 159 Wells Avenue, Newton, MA 02459, USA. gli1@partners.org (G. Li).

contact biomechanics research, and may provide guidelines for development of anatomical total knee arthroplasties that are aimed to reproduce normal knee joint kinematics

Keywords

Knee; cartilage; in-vivo kinematics; step up motion; cartilage contact; contact geometry

Introduction

Accurate knowledge of articular cartilage contact kinematics is critical for investigation of knee joint function and for development of surgical modalities to treat knee pathology such as using cartilage repair and partial or total knee arthroplasty (Bonnin et al., 2016; Henak et al., 2013; Liu et al., 2010; Lunebourg et al., 2016). Numerous studies have investigated the tibiofemoral cartilage contact using both in-vitro and in-vivo experimental set ups, including cadaveric knee tests (D'Agata et al., 1993; Guettler et al., 2005), in silico three dimensional (3D) knee joint modeling (Halonen et al., 2014; Shim et al., 2016), in-vivo imaging measurements (Bingham et al., 2008; Carter et al., 2015; Chan et al., 2016; Coleman et al., 2013; Eckstein et al., 2005; Henak et al., 2013; Kaiser et al., 2016; Lad et al., 2016; Liu et al., 2010; Sutter et al., 2015). While these studies have greatly advanced our knowledge on human knee joint biomechanics, no data has been reported on the articular surface geometry at the contact locations.

The articular surface geometry at the contact area is an important variable that affects the articular contact behaviors, such as contact stress and knee joint stability. In literature, few studies have analyzed the complicated geometry of the tibial and femoral cartilage surfaces using cadaveric knee specimens (Ateshian et al., 1991; Cohen et al., 1999). These studies measured the surface morphology of the knee, including the tibial and femoral dimensions and shape (represented by the ratio of anteroposterior and mediolateral dimensions) (Kurosawa et al., 1985; Mahfouz et al., 2012). However, due to the challenge in measurement technologies, it is difficult to determine local cartilage surface shape at the articular contact locations during in-vivo physiological activities of the knee. This information is instrumental for development of surgical strategies to treat cartilage related pathologies that are aimed to repair tibiofemoral articular surfaces (such as using cartilage repair and partial or total knee arthroplasty) and to restore normal knee joint function (Henak et al., 2013; Nagerl et al., 2015; Walker and Sathasivam, 2000; Walker et al., 2010).

Therefore, the objective of this study was to investigate the surface geometry at the articular contact areas of the tibiofemoral joint during a dynamic functional activity of the knee. Since previous studies showed that the cartilage contact areas and thicknesses are different at the medial and lateral compartments during functional activities of the knee (Bingham et al., 2008; Liu et al., 2010), we hypothesized that the articular surface geometries at the medial and lateral compartments of the tibiofemoral joint are different in the areas of in-vivo articular cartilage contact.

Material and methods

Subject selection

The study was approved by our Institutional Review Board. Ten healthy knees of 5 male and 5 female subjects with no history of previous knee injury and joint pathology symptoms (confirmed by physical examination and MR images acquired during experiment) were tested in this study. These subjects were 36.7 ± 9.3 years old and with a body mass index of 25.5 ± 2.8 kg/m^2. Written consent was obtained from all the subjects prior to participation in this study.

MRI and dual fluoroscopic imaging procedures

All the subjects were (magnetic resonance) MR scanned using a 3-Tesla scanner (MAGNETOM Trio, Siemens, Malvern, PA, USA) with a surface coil and a fat-suppressed, double-echo water excitation sequence (field of view: 160mm×160mm, image resolution: 512×512, voxel size: 0.31mm×0.31mm×1.00mm, time of repetition: 24ms, time of echo: 6.5ms and flip angle: 25°, imaging time: 12 minutes). The MR images were used to construct a three-dimensional (3D) model of the knee including femur, tibia, and their cartilage surfaces in solid modelling software (Rhinoceros, Robert McNeel & Associates, Seattle, WA, USA) using an established protocol of our lab.

A combined dual fluoroscopic imaging system (DFIS) and 3D MR imaging based modeling technique was used to capture the knee motion during a dynamic step-up activity. The accuracy of the technique on reproducing knee and cartilage contact kinematics have been extensively validated previously (Bingham et al., 2008; Li et al., 2008; Liu et al., 2010; Wan et al., 2008). The speed of the step-up activity was not controlled. Each subject performed the step-up in his/her own natural way. The initiation of the knee motion during the step-up motion (foot touching the step) was defined as 0%, and the fully extended knee position was defined as 100% of the step-up motion. The mean maximum flexion angle at the initiation (0%) of the step-up motion was 56.9±5.5° and 1.6±4.1° at the end (100%) of the motion. Kinematics of the knee was analyzed at every 10% of the activity using the fluoroscopic images and the 3D bone models through a 2D–3D matching process (DeFrate et al., 2004). The corresponding cartilage models were mapped to the bone models at every knee position to analyze the in-vivo cartilage contact kinematics.

Cartilage contact biomechanics

Cartilage contact area was defined as the overlapping of the tibial and femoral cartilage surfaces (Liu et al., 2010). Cartilage deformation (%) was defined as the penetration of cartilage mesh models (mm) divided by the sum of the tibia and femur cartilage thickness (mm) and multiplied by 100 (Liu et al., 2010). The overall peak cartilage deformation locations were defined as the locations of the peak cartilage deformation along the step-up motion path. To quantitatively describe the cartilage contact locations on the femoral condyles, two radial coordinated systems were created using the femoral condyle anatomy (Bingham et al., 2008; Liu et al., 2010), where both the contact angle (α) (Fig. 1A) in the sagittal plane and deviation angle (β) (Fig. 1B) in the plane perpendicular to the sagittal plane were measured. The contact angle was defined as the angle between the femoral long

axis (parallel to the posterior wall of the femoral shaft) and the sagittal plane condyle radius; the deviation angle was measured between the radius passing the contact point and the lowest point of the fitting circle of the condyle surface in the plane perpendicular to the sagittal plane.

To quantify the cartilage contact location on the tibial plateau, a coordinate system was created, which has been described in detail in a previous study (Fig. 1C) (Li et al., 2005; Liu et al., 2010). The tibial long axis was defined as the line parallel to the posterior wall of the tibia shaft. The medial-lateral (ML) axis was defined as a line connecting the centroids of the two circles fitted to the posterior edge of the medial and lateral tibial plateau surfaces. The anterior-posterior (AP) axis was perpendicular to the above mentioned two axes. In the ML direction, a location lateral to the AP axis was considered positive. In the AP direction, a location anterior to the ML axis was considered positive. The knee flexion angle was measured as the angle between the tibial and femoral long axes in the sagittal plane.

Cartilage contact area geometry

The geometry of the cartilage contact area on the tibial plateau surface was analyzed using the curvature of the cartilage surface geometry at the peak cartilage contact deformation location. Two orthogonal sectional planes, sagittal and coronal, were created at each peak contact deformation location along the step-up motion path. The profiles of the tibial and femoral cartilage in the contact area on these two planes were fitted using circles and the radii were measured (Fig. 2). For tibial cartilage, if the tibiofemoral cartilage is in a conforming contact, i.e., its curvature was in the same direction of the femoral cartilage, the radius value was defined as positive; if the tibiofemoral cartilage is in a convex contact, i.e., its curvature was in the opposite direction of the femoral cartilage, the radius value of the tibial cartilage was defined as negative.

Statistical analysis

A repeated measure analysis of variance (ANOVA) and a post-hoc Student-Newman-Keuls test were used to determine statistical difference in cartilage contact locations and contact area radii at different time points along the step-up motion path and between medial and lateral compartments during the step-up motion. A statistically significant difference was determined when $p<0.05$.

Results

Cartilage contact location

The mean maximum flexion angle at the initiation (0%) of the step-up motion was 56.9±5.5° and 1.6±4.1° at the end (100%) of the motion. The peak contact deformation locations at medial and lateral femoral condyles moved anteriorly and were located at the intercondylar side of the femoral cartilage (Table 1). The total range of contact angle (α) on the medial femoral condyle (71.1±5.3°) was significantly larger than that on the lateral condyle (61.8±2.2°) ($P<0.001$). The total range of deviation angle (β) was significantly smaller on the medial (8.4±2.4°) than on the lateral (10.4±1.9°) condyles ($P=0.04$).

On the tibial plateau, the peak contact deformation locations shifted posteriorly from 0% to 30% of the step-up motion at both the medial and lateral compartments, and then consistently moved anteriorly from 30% to 100% (Table 2). In the medial-lateral direction, the peak contact locations moved away from the tibial spine area from 0% to 30% of the step-up motion, and then moved towards the tibial spine area from 30% to 100%. The cartilage contact excursions in anteroposterior and mediolateral directions on the tibia plateau were similar in the medial (AP, 7.2±2.0 mm; ML, 6.4±2.2 mm) and lateral (AP, 7.1±1.9 mm; ML, 6.2±2.0 mm) compartments ($p>0.05$).

Cartilage surface geometry at the contact area

Sagittal plane—The sagittal radius of the contact area in the medial femoral cartilage was 23.4±3.1 mm at the beginning of step-up motion, and increased to 27.7±3.8 mm at 40% (Fig. 3A). It then consistently increased to 33.9±4.5 mm at 80% and slightly dropped down until 100%. The sagittal radius in the medial tibial cartilage was −60.5±17.8mm at 0% of the step-up motion. It then increased consistently to −141.2±31.3 mm at 40% of the motion (Fig. 3B) and after 40%, the sagittal radius consistently changed to −38.0±66.5 mm at 100%.

The sagittal radius of the contact area in the lateral femoral condyle cartilage was 18.2±3.3mm at the beginning of the step-up motion, and increased to 20.6±3.6 mm at 40% (Fig. 3A). It then consistently increased to 29.6±3.8 until 90% and then slightly dropped down until 100%. The sagittal radius in the lateral tibial cartilage was −37.6±4.5mm at 0% (Fig. 3B). It then increased consistently to −56.9±38.8 at 30%. After 30%, it decreased with extension and dropped to −37.8±11.6 mm at 100%.

Coronal plane—The coronal plane radius of the contact area in the medial femoral cartilage was 19.8±4.4 mm at 0% of the step-up motion, and increased to 20.8±4.1 mm at 40% (Fig. 3C). It only slightly changed until 100%. The coronal radius in medial tibial cartilage was 26.9±6.1 mm at 0% of the step-up motion (Fig. 3D). It increased consistently to 36.7±11.4 mm at 40%. Beyond 40%, the coronal radius decreased to 29.3±7.8 mm at 100%.

The coronal radius in the lateral femoral condyle cartilage was 18.2±3.3mm at 0% of the step-up motion, and increased to 20.6±3.6 mm at 40% (Fig. 3C). It then slightly changes until 100%. The coronal radius in lateral tibial cartilage was 37.6±4.5mm at 0% of the step-up motion and kept increasing until 40% (47.4±8.5 mm) (Fig. 3D). It then consistently decreased to 34.6±5.9mm at 100%.

Comparison of medial and lateral compartments

The mean sagittal radius of the femur cartilage was larger in the medial side than in the lateral side ($P<0.001$). No significant difference was found in the mean coronal radii of the medial and lateral femoral cartilage ($P=0.27$). The mean sagittal radius in the tibia cartilage was larger in medial compartment than the lateral compartment ($P<0.001$). The average coronal radius in tibia cartilage was smaller in medial compartment than in the lateral compartment ($P<0.001$).

Discussion

The principal finding of this study was that both medial and lateral compartments were under convex (femur) to convex (tibia) cartilage contact in the sagittal plane, where the radius of the medial tibial articular surface was larger than the lateral tibial side. Our study also found that both medial and lateral cartilage contact locations moved anteriorly on the tibia and move toward the intercondylar part of the femur and tibia during the step-up motion. These data indicate that the medial and lateral tibiofemoral cartilage contact geometries were similar in patterns, but different in dimensions, and therefore, were partially consistent with our study hypothesis.

In general, our data on cartilage contact kinematics during the step-up motion are consistent with those reported in literature during various functional activities. For example, many studies have reported on cartilage contact locations on tibial plateau using various technologies (Bingham et al., 2008; DeFrate et al., 2004; Kaiser et al., 2016; Liu et al., 2010). These studies revealed that medial contact locations were more anteriorly than the lateral side. Few studies also indicated that the cartilage contact locations on the femoral condyle were located at the inner part of the condylar cartilage (Bingham et al., 2008; Li et al., 2013; Liu et al., 2010). However, a direct comparison between different studies is difficult since the knee experiences different loading conditions during different activities among these studies.

The observation on convex-to-convex tibiofemoral cartilage contact in sagittal plane at both the medial and lateral compartments may provide important insights into the investigation of intrinsic articular contact biomechanics of the knee. This geometric feature of the articular contact area in medial compartment indicates that the femur is less constrained by the tibial cartilage surface geometry in the anteroposterior direction than a convex-to-concave contact in the medial-lateral direction. Therefore, the convex-to-convex contact feature implies that the dynamic stability of the knee joint could depend on a synergistic interaction of articular contact, mechanical function of the meniscus, ligament constraints (such as the cruciate and collateral ligaments), muscle contractions and other tissues around the knee joint (Rao et al., 2015; Reynolds et al., 2017; Wang et al., 2016; Zhu et al., 2017). Dysfunction of any of these structural components could cause alteration of articular contact biomechanics of the knee and possibly result in damage to the cartilage. It is warranted to investigate the effect of various injuries to the knee joint, such as ligament or meniscus tears, on the articular cartilage contact characters during functional knee joint activities.

In knee arthroplasty surgeries, majority of the total knee replacement component designs have also adopted a femoral convex to tibia concave contact concept (De Valk et al., 2016; Nagerl et al., 2015; Walker and Sathasivam, 2000; Walker et al., 2010). Recently, medial pivoting knee motion has also been adopted in several knee replacement designs that are aimed to reproduce anatomic knee joint motion patterns (Chinzei et al., 2014; Ishida et al., 2012; Morra et al., 2008; Pritchett, 2011; Schmidt et al., 2003; Schmidt et al., 2014). However, our data showed that both the medial and lateral cartilage contacts are a convex femur to a convex tibia contact in sagittal plane. Further, the excursions of the contact points on the medial and lateral sides were similar along the anteroposterior and mediolateral

directions on the tibial plateau surface, which does not indicate a medial or lateral pivoting motion pattern of the knee during the step-up motion. Knee joint kinematics may be activity dependent and contemporary knee replacement designs need to consider knee function in a variety of functional activities. Our data could provide a useful reference for development of new concepts in anatomic knee joint replacements that are aimed to mimic normal knee joint motion (Varadarajan et al., 2015).

There are several limitations in our study that should be noted when interpreting the data. First, the DFIS cannot image the meniscus motion. Therefore, it is not possible to determine the in-vivo meniscus-cartilage contact in response to physiological loading conditions. Future studies may use dynamic MR imaging technologies to determine functional activities of the meniscus-cartilage contact. Second, overlap of tibiofemoral cartilage surfaces was used to calculate cartilage contact areas. This method may underestimate the actual cartilage contact area because that the actual cartilage surfaces do not penetrate into each other during the articular contact. Futures studies should use the cartilage contact kinematics as boundary conditions to calculate actual cartilage contact deformation. Third, only step-up activity was investigated. Future studies should investigate the articular contact patterns during other daily functional activities, such as walking, running, squatting, to determine the cartilage contact characters under various physiological loading conditions. Nevertheless, we believe that the data reported in this paper provides an important reference in normal in-vivo tibiofemoral cartilage contact biomechanics.

In conclusion, we found that both medial and lateral compartments were under convex (femur) to convex (tibia) contact in the sagittal plane; the medial tibial articular contact radius was larger than the lateral side. Our results also indicated that the excursions of the cartilage locations were similar in the medial and lateral compartments during the step-up motion. These data provide insights into the in-vivo physiological function of the articular cartilage, and could be an important reference for development of anatomic total knee arthroplasty that is aimed to reproduce normal knee joint kinematics.

Acknowledgments

This work was supported by National Institute of Health Grant (R01AR055612) and China Scholarship Council (CSC201506200012).

References

Ateshian GA, Soslowsky LJ, Mow VC. Quantitation of articular surface topography and cartilage thickness in knee joints using stereophotogrammetry. Journal of biomechanics. 1991; 24:761–776. [PubMed: 1918099]

Bingham JT, Papannagari R, Van de Velde SK, Gross C, Gill TJ, Felson DT, Rubash HE, Li G. In vivo cartilage contact deformation in the healthy human tibiofemoral joint. Rheumatology (Oxford, England). 2008; 47:1622–1627.

Bonnin MP, Saffarini M, Bossard N, Dantony E, Victor J. Morphometric analysis of the distal femur in total knee arthroplasty and native knees. The bone & joint journal. 2016; 98-b:49–57. [PubMed: 26733515]

Carter TE, Taylor KA, Spritzer CE, Utturkar GM, Taylor DC, Moorman CT 3rd, Garrett WE, Guilak F, McNulty AL, DeFrate LE. In vivo cartilage strain increases following medial meniscal tear and

correlates with synovial fluid matrix metalloproteinase activity. Journal of biomechanics. 2015; 48:1461–1468. [PubMed: 25801424]

Chan DD, Cai L, Butz KD, Trippel SB, Nauman EA, Neu CP. In vivo articular cartilage deformation: noninvasive quantification of intratissue strain during joint contact in the human knee. Scientific reports. 2016; 6:19220. [PubMed: 26752228]

Chinzei N, Ishida K, Matsumoto T, Kuroda Y, Kitagawa A, Kuroda R, Akisue T, Nishida K, Kurosaka M, Tsumura N. Evaluation of patellofemoral joint in ADVANCE Medial-pivot total knee arthroplasty. International orthopaedics. 2014; 38:509–515. [PubMed: 23925880]

Cohen ZA, McCarthy DM, Kwak SD, Legrand P, Fogarasi F, Ciaccio EJ, Ateshian GA. Knee cartilage topography, thickness, and contact areas from MRI: in-vitro calibration and in-vivo measurements. Osteoarthritis and cartilage. 1999; 7:95–109. [PubMed: 10367018]

Coleman JL, Widmyer MR, Leddy HA, Utturkar GM, Spritzer CE, Moorman CT 3rd, Guilak F, DeFrate LE. Diurnal variations in articular cartilage thickness and strain in the human knee. Journal of biomechanics. 2013; 46:541–547. [PubMed: 23102493]

D'Agata SD, Pearsall AWt, Reider B, Draganich LF. An in vitro analysis of patellofemoral contact areas and pressures following procurement of the central one-third patellar tendon. The American journal of sports medicine. 1993; 21:212–219. [PubMed: 8465915]

De Valk EJ, Noorduyn JC, Mutsaerts EL. How to assess femoral and tibial component rotation after total knee arthroplasty with computed tomography: a systematic review. Knee surgery, sports traumatology, arthroscopy : official journal of the ESSKA. 2016; 24:3517–3528.

DeFrate LE, Sun H, Gill TJ, Rubash HE, Li G. In vivo tibiofemoral contact analysis using 3D MRI-based knee models. Journal of biomechanics. 2004; 37:1499–1504. [PubMed: 15336924]

Eckstein F, Lemberger B, Gratzke C, Hudelmaier M, Glaser C, Englmeier KH, Reiser M. In vivo cartilage deformation after different types of activity and its dependence on physical training status. Annals of the rheumatic diseases. 2005; 64:291–295. [PubMed: 15647438]

Guettler JH, Demetropoulos CK, Yang KH, Jurist KA. Dynamic evaluation of contact pressure and the effects of graft harvest with subsequent lateral release at osteochondral donor sites in the knee. Arthroscopy : the journal of arthroscopic & related surgery : official publication of the Arthroscopy Association of North America and the International Arthroscopy Association. 2005; 21:715–720.

Halonen KS, Mononen ME, Jurvelin JS, Toyras J, Salo J, Korhonen RK. Deformation of articular cartilage during static loading of a knee joint--experimental and finite element analysis. Journal of biomechanics. 2014; 47:2467–2474. [PubMed: 24813824]

Henak CR, Anderson AE, Weiss JA. Subject-specific analysis of joint contact mechanics: application to the study of osteoarthritis and surgical planning. Journal of biomechanical engineering. 2013; 135:021003. [PubMed: 23445048]

Ishida K, Matsumoto T, Tsumura N, Chinzei N, Kitagawa A, Kubo S, Chin T, Iguchi T, Akisue T, Nishida K, Kurosaka M, Kuroda R. In vivo comparisons of patellofemoral kinematics before and after ADVANCE Medial-Pivot total knee arthroplasty. International orthopaedics. 2012; 36:2073–2077. [PubMed: 22885803]

Kaiser J, Vignos MF, Liu F, Kijowski R, Thelen DG. American Society of Biomechanics Clinical Biomechanics Award 2015: MRI assessments of cartilage mechanics, morphology and composition following reconstruction of the anterior cruciate ligament. Clinical biomechanics (Bristol, Avon). 2016; 34:38–44.

Kurosawa H, Walker PS, Abe S, Garg A, Hunter T. Geometry and motion of the knee for implant and orthotic design. Journal of biomechanics. 1985; 18:487–499. [PubMed: 4030805]

Lad NK, Liu B, Ganapathy PK, Utturkar GM, Sutter EG, Moorman CT 3rd, Garrett WE, Spritzer CE, DeFrate LE. Effect of normal gait on in vivo tibiofemoral cartilage strains. Journal of biomechanics. 2016; 49:2870–2876. [PubMed: 27421206]

Li G, DeFrate LE, Park SE, Gill TJ, Rubash HE. In vivo articular cartilage contact kinematics of the knee: an investigation using dual-orthogonal fluoroscopy and magnetic resonance image-based computer models. The American journal of sports medicine. 2005; 33:102–107. [PubMed: 15611005]

Li G, Van de Velde SK, Bingham JT. Validation of a non-invasive fluoroscopic imaging technique for the measurement of dynamic knee joint motion. Journal of biomechanics. 2008; 41:1616–1622. [PubMed: 18394629]

Li JS, Hosseini A, Cancre L, Ryan N, Rubash HE, Li G. Kinematic characteristics of the tibiofemoral joint during a step-up activity. Gait & posture. 2013; 38:712–716. [PubMed: 23541765]

Liu F, Kozanek M, Hosseini A, Van de Velde SK, Gill TJ, Rubash HE, Li G. In vivo tibiofemoral cartilage deformation during the stance phase of gait. Journal of biomechanics. 2010; 43:658–665. [PubMed: 19896131]

Lunebourg A, Parratte S, Galland A, Lecuire F, Ollivier M, Argenson JN. Is isolated insert exchange a valuable choice for polyethylene wear in metal-backed unicompartmental knee arthroplasty? Knee surgery, sports traumatology, arthroscopy : official journal of the ESSKA. 2016; 24:3280–3286.

Mahfouz M, Abdel Fatah EE, Bowers LS, Scuderi G. Three-dimensional morphology of the knee reveals ethnic differences. Clinical orthopaedics and related research. 2012; 470:172–185. [PubMed: 21948324]

Morra EA, Rosca M, Greenwald JF, Greenwald AS. The influence of contemporary knee design on high flexion: a kinematic comparison with the normal knee. The Journal of bone and joint surgery. American. 2008; 90(Suppl 4):195–201.

Nagerl H, Dathe H, Fiedler C, Gowers L, Kirsch S, Kubein-Meesenburg D, Dumont C, Wachowski MM. The morphology of the articular surfaces of biological knee joints provides essential guidance for the construction of functional knee endoprostheses. Acta of bioengineering and biomechanics. 2015; 17:45–53. [PubMed: 26400423]

Pritchett JW. Patients prefer a bicruciate-retaining or the medial pivot total knee prosthesis. The Journal of arthroplasty. 2011; 26:224–228. [PubMed: 20932707]

Rao AJ, Erickson BJ, Cvetanovich GL, Yanke AB, Bach BR Jr, Cole BJ. The Meniscus-Deficient Knee: Biomechanics, Evaluation, and Treatment Options. Orthopaedic journal of sports medicine. 2015; 3 2325967115611386.

Reynolds RJ, Walker PS, Buza J. Mechanisms of anterior-posterior stability of the knee joint under load-bearing. Journal of biomechanics. 2017; 57:39–45. [PubMed: 28433391]

Schmidt R, Komistek RD, Blaha JD, Penenberg BL, Maloney WJ. Fluoroscopic analyses of cruciate-retaining and medial pivot knee implants. Clinical orthopaedics and related research. 2003:139–147.

Schmidt R, Ogden S, Blaha JD, Alexander A, Fitch DA, Barnes CL. Midterm clinical and radiographic results of the medial pivot total knee system. International orthopaedics. 2014; 38:2495–2498. [PubMed: 25011412]

Shim VB, Besier TF, Lloyd DG, Mithraratne K, Fernandez JF. The influence and biomechanical role of cartilage split line pattern on tibiofemoral cartilage stress distribution during the stance phase of gait. Biomechanics and modeling in mechanobiology. 2016; 15:195–204. [PubMed: 25861029]

Sutter EG, Widmyer MR, Utturkar GM, Spritzer CE, Garrett WE Jr, DeFrate LE. In vivo measurement of localized tibiofemoral cartilage strains in response to dynamic activity. The American journal of sports medicine. 2015; 43:370–376. [PubMed: 25504809]

Varadarajan KM, Zumbrunn T, Rubash HE, Malchau H, Muratoglu OK, Li G. Reverse Engineering Nature to Design Biomimetic Total Knee Implants. The journal of knee surgery. 2015; 28:363–369. [PubMed: 26166428]

Walker PS, Sathasivam S. Design forms of total knee replacement. Proceedings of the Institution of Mechanical Engineers. Part H, Journal of engineering in medicine. 2000; 214:101–119.

Walker PS, Yildirim G, Arno S, Heller Y. Future directions in knee replacement. Proceedings of the Institution of Mechanical Engineers. Part H, Journal of engineering in medicine. 2010; 224:393–414.

Wan L, de Asla RJ, Rubash HE, Li G. In vivo cartilage contact deformation of human ankle joints under full body weight. Journal of orthopaedic research : official publication of the Orthopaedic Research Society. 2008; 26:1081–1089. [PubMed: 18327792]

Wang X, Malik A, Bartel DL, Wright TM, Padgett DE. Load Sharing Among Collateral Ligaments, Articular Surfaces, and the Tibial Post in Constrained Condylar Knee Arthroplasty. Journal of biomechanical engineering. 2016; 138

Zhu J, Dong J, Marshall B, Linde MA, Smolinski P, Fu FH. Medial collateral ligament reconstruction is necessary to restore anterior stability with anterior cruciate and medial collateral ligament injury. Knee surgery, sports traumatology, arthroscopy : official journal of the ESSKA. 2017

Highlights

1. Both medial and lateral sides of the knee were under convex to convex contact in sagittal plane.
2. Tibiofemoral contact locations moved toward the intercondylar areas during the step-up motion.
3. Medial and lateral cartilage contact geometries were similar in pattern, different in dimension.

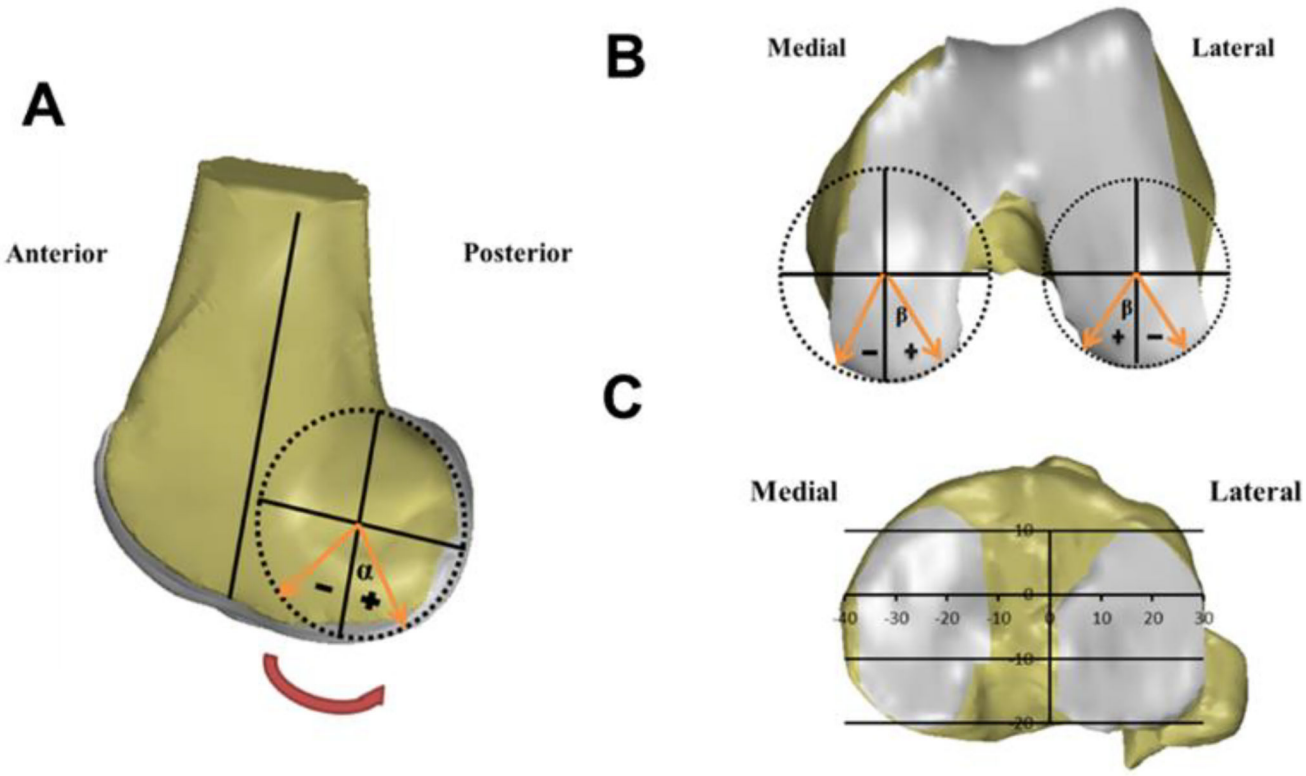

Fig.1.

The definition for measurement of the (A) contact angle (α) and (B) deviation angle (β) on the femoral condyle cartilage surface, and (C) the coordinate system for measurement of cartilage contact locations on the tibial plateau.

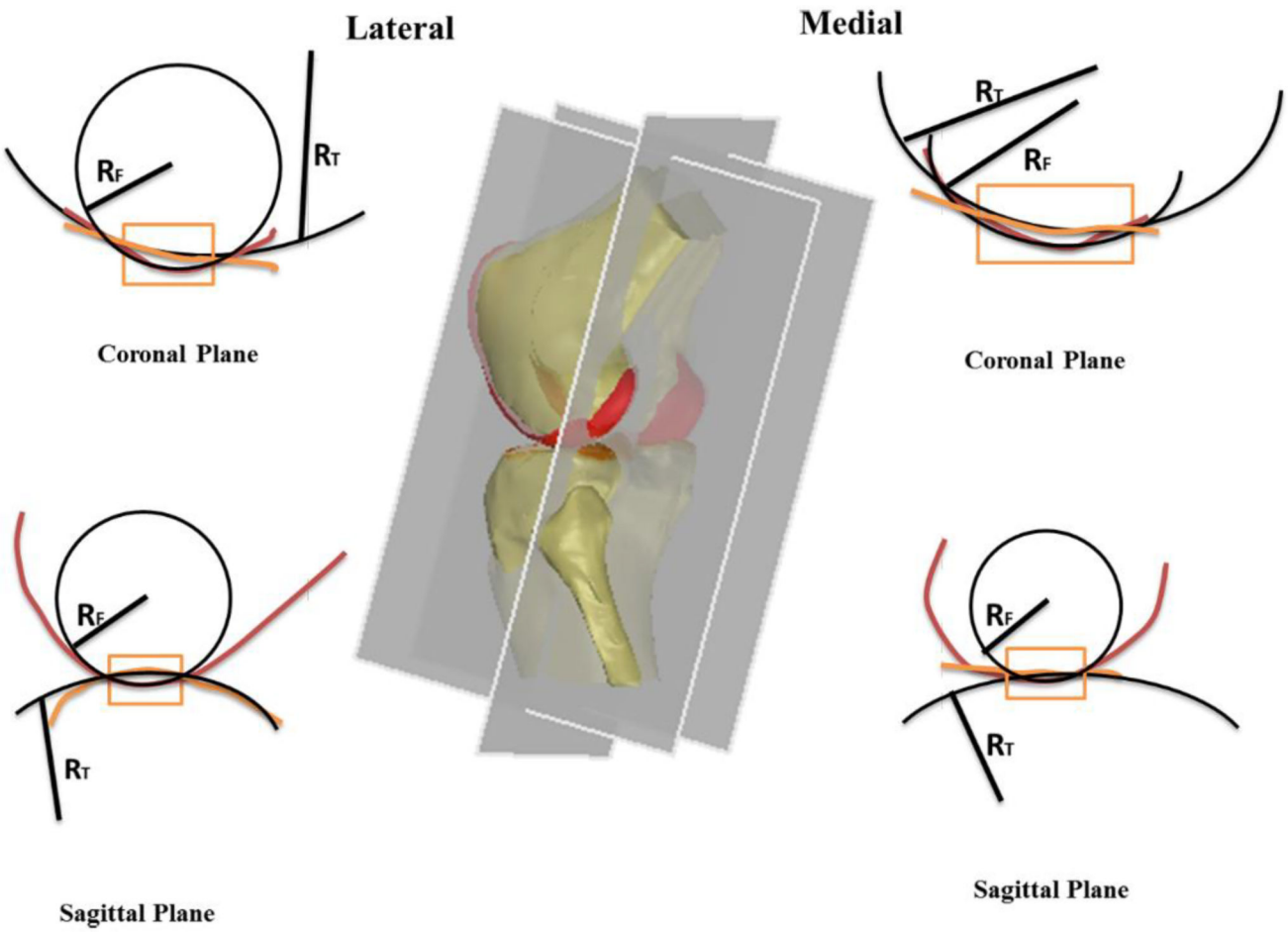

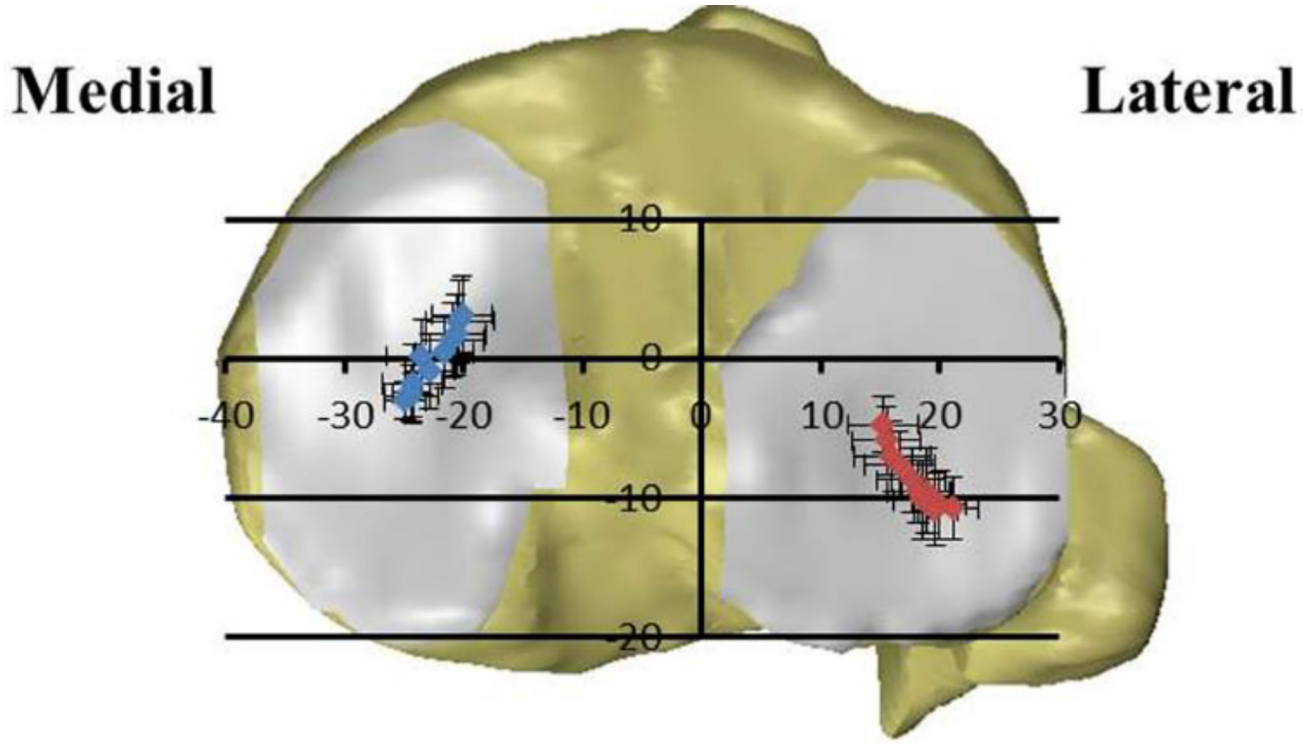

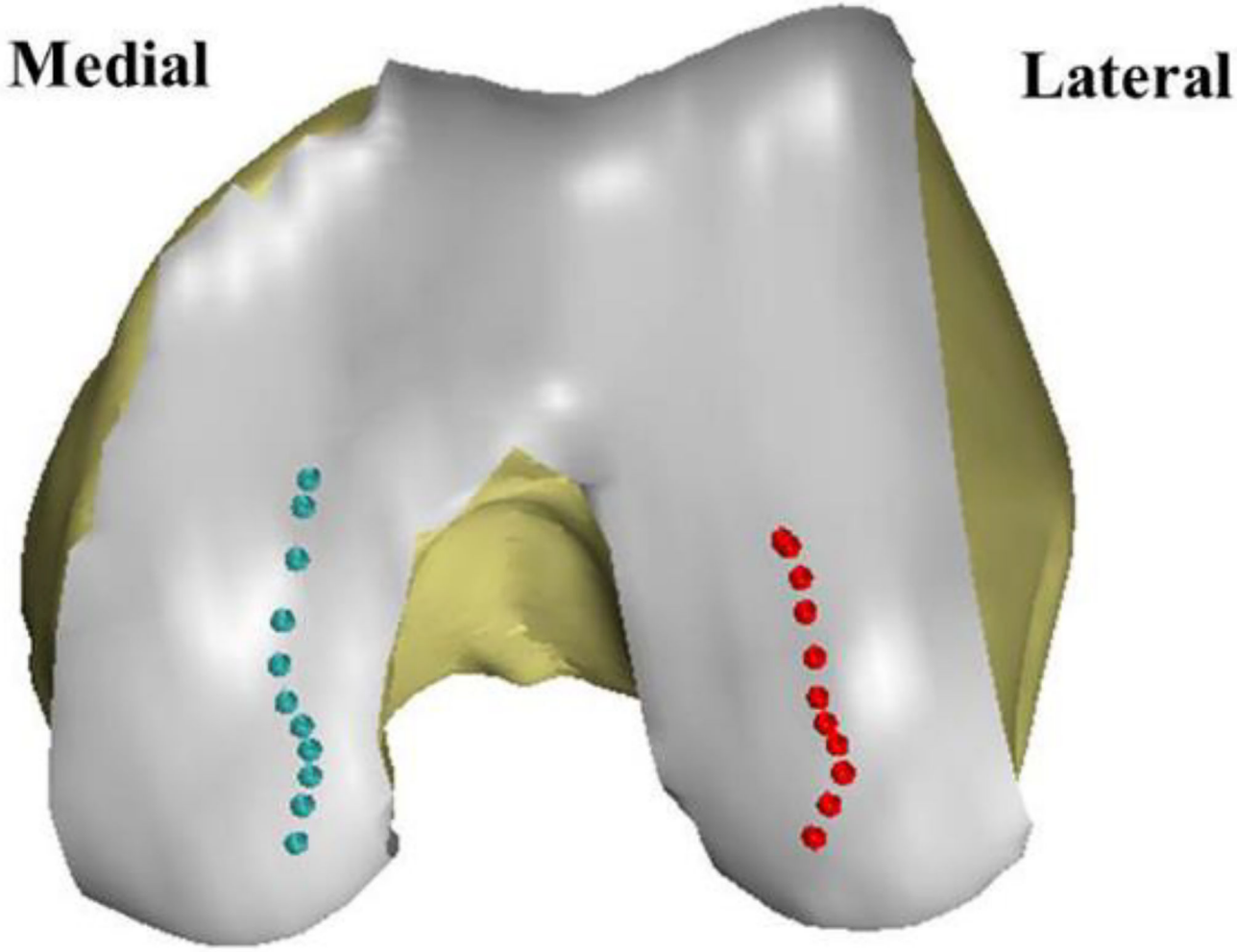

Fig.2.
Schematic diagrams showing the measurement of cartilage surface geometry at the contact areas in the sagittal and coronal planes.

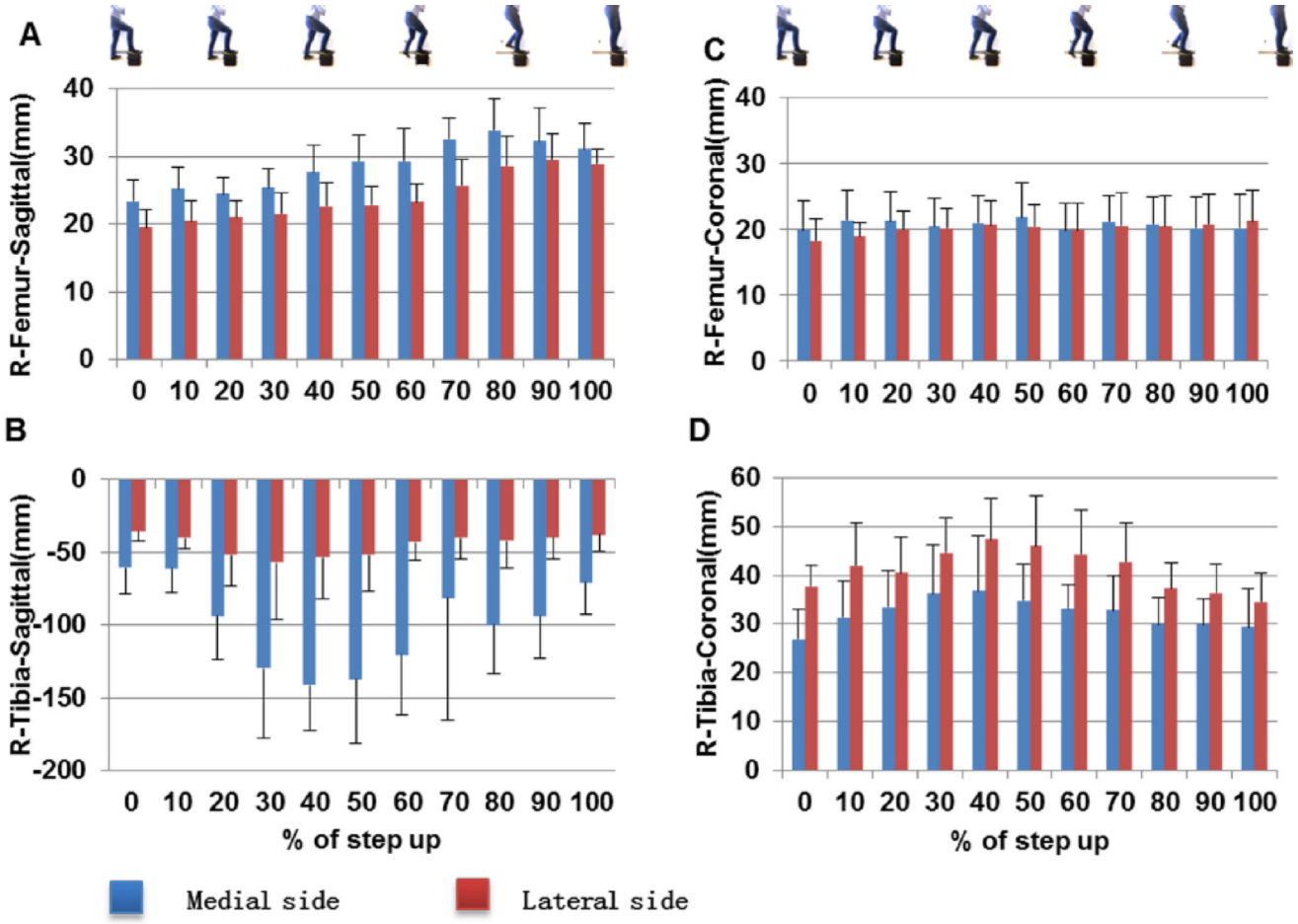

Fig.3.

The radii of the contact areas in both medial and lateral cartilage surfaces in sagittal (A) femur and (B) tibia cartilages; and in coronal (C) femur and (D) tibia surfaces of the knee.

Table 1

The femoral contact angle (α) and deviation angle (β) in the medial and lateral compartments

Percent	Medial-α (°) Mean (SD)	Medial-β(°) Mean (SD)	Lateral-α(°) Mean (SD)	Lateral-β(°) Mean (SD)
0%	47.4 (4.2)	8.0 (1.7)	46.4 (2.0)	10.9 (1.6)
10%	37.9 (4.5)	9.6 (1.4)	38.7 (3.5)	7.8 (3.0)
20%	31.3 (5.9)	11.4 (1.3)	32.3 (5.3)	5.1 (2.4)
30%	25.4 (6.6)	11.5 (2.0)	27.0 (5.6)	6.0 (2.3)
40%	20.1 (6.3)	10.1 (3.7)	23.1 (5.0)	7.9 (2.7)
50%	15.1 (6.2)	7.3 (3.8)	18.3 (6.0)	9.2 (3.7)
60%	7.7 (6.3)	6.1 (3.0)	10.7 (7.4)	9.5 (3.3)
70%	−0.3 (8.4)	6.9 (1.8)	2.0 (8.6)	10.9 (2.9)
80%	−10.6 (7.0)	9.4 (1.5)	−4.3 (6.4)	11.4 (2.4)
90%	−18.9 (6.4)	10.3 (1.0)	−10.7 (6.0)	13.4 (1.8)
100%	−23.2 (4.5)	11.1 (1.3)	−14.5 (2.4)	14.6 (2.3)
Total range	71.1 (5.3)	8.4 (2.4)	61.8 (2.2)	10.4 (1.9)

Table 2

Cartilage contact locations on the tibia plateau in the AP and ML directions

Percent	Medial-AP(mm) Mean (SD)	Medial-ML(mm) Mean (SD)	Lateral-AP(mm) Mean (SD)	Lateral-ML(mm) Mean (SD)
0%	0.2 (2.7)	−23.4 (3.0)	−9.5 (3.1)	19.0 (2.1)
10%	−1.8 (2.8)	−24.2 (2.5)	−10.5 (2.4)	20.1 (2.2)
20%	−2.6 (1.6)	−24.3 (2.3)	−10.8 (2.2)	21.1 (2.1)
30%	−3.1 (1.3)	−24.9 (1.7)	−10.9 (2.6)	19.7 (1.8)
40%	−2.5 (2.0)	−24.3 (1.6)	−10.1 (2.8)	18.6 (2.5)
50%	−0.9 (2.7)	−22.8 (2.1)	−9.5 (2.2)	18.3 (2.7)
60%	0.5 (2.5)	−21.6 (2.5)	−8.7 (2.3)	17.7 (2.9)
70%	1.3 (2.7)	−20.9 (2.6)	−7.6 (2.4)	16.6 (3.0)
80%	1.7 (2.9)	−20.6 (2.6)	−7.0 (2.6)	16.1 (3.2)
90%	2.7 (3.0)	−20.3 (2.9)	−5.9 (2.4)	15.6 (2.8)
100%	3.1 (2.8)	−20.1 (2.6)	−4.7 (2.0)	15.3 (3.0)
Total range	7.2 (2.0)	6.4 (2.2)	7.1 (1.9)	6.2 (2.0)

AP Anterior-Posterior **ML** Medial-Lateral